A nonlinear switched control strategy for permanent magnet synchronous machines

Lucas N. Egidio, Grace S. Deaecto, João P. Hespanha, José C. Geromel

Abstract— **A novel approach for controlling permanent magnet synchronous machines (PMSMs) based on switched systems theory is presented in this paper. The PMSM is generally fed by a three-phase voltage source inverter with six electronic switches whose control is responsible for orchestrating the machine shaft velocity towards a desired steady-state value. This assembly is modeled as a nonlinear switched system characterized by sinusoidal functions of the machine shaft displacement, whose properties are suitably explored in order to obtain the control design conditions. Our main goal is to design a state dependent switching function for this class of switched nonlinear systems to assure asymptotic stability and a maximum guaranteed decay rate for the closed-loop system. The design is based on a non-quadratic Lyapunov function and the stability conditions are expressed in the form of a generalized eigenvalue minimization problem. A simulation example is used to show the efficiency of the proposed control methodology as well as to discuss future work.**

I. INTRODUCTION

Several strategies dealing with the control of permanent magnet synchronous machines (PMSMs) have been developed throughout the last decades. These machines can be described as electrical drives with a rotor that possesses permanent magnets and a set of windings in the stator that are responsible for creating an appropriate magnetic flux to generate the desired torque and/or velocity. See [15] for an extensive study on these machines. PMSMs are often connected to a voltage source inverter with switches capable of commanding a desired voltage level to each phase terminal. Two main strategies to control the switching pattern can be highlighted from the literature, namely, field-oriented control (FOC) and direct torque control (DTC). The former generally takes into account a set of pulse-width modulation (PWM) signals that control the average of each phase voltage. This strategy regulates the phase currents and, consequently, the machine torque. The DTC approach selects the switch states through a predefined table, based on torque and flux error signals. Detailed analyses of these control schemes can be found, e.g., in [3], [15] and [19].

In both schemes the dynamic behavior of this assembly is often modeled using auxiliary reference frames, see [15]. These reference frames, described by means of Clarke and Park transformations, allow the nonlinear model to be rewritten in an alternative manner that may ease the design of controllers. These techniques generally rely upon the existence of an outer control loop for commanding a suitable reference torque, bringing the rotor velocity to a desired steady-state value. In the present paper, instead, we adopt the original nonlinear model, without using any auxiliary reference frame, and propose a control methodology based on a unique control loop.

Switched systems consist of a set of subsystems, often called operation modes, and a switching function (or rule) that activates one of them at each instant of time. Some basic references on this theme are [8], [12], [16] and [17]. Switched affine systems are an important subclass which can be used to model a great number of systems in the power electronics domain, see for instance, [4] and [10]. These systems are characterized by the existence of several equilibrium points that can be attained by the action of a state or output-dependent switching function. In this framework, references [1], [5], [7], and [18] deal with the switching function control design in the continuous-time domain, assuring asymptotic stability of a desired equilibrium point, while [6] and [11] address the discrete-time domain and assure practical stability. The class of systems that we consider in this paper is more general, since besides the presence of affine terms, the dynamical model is represented by a set of coupled nonlinear differential equations containing sinusoidal functions.

This paper addresses the rotational velocity regulation of a PMSM within the framework of switched systems, by continuously deciding whether each electronic switch in a three-phase voltage inverter should be open or closed. The assembly is modeled as a switched nonlinear system and our main goal is to design a state dependent switching function assuring asymptotic stability and a maximum decay rate for the closed-loop system. Our approach is based on a non-quadratic Lyapunov function that takes advantage of the trigonometric properties of the sinusoidal functions appearing in the dynamical model of the machine. The design of the switching function involves the solution of a generalized eigenvalue minimization problem [2]. The validity and efficiency of the proposed design method are illustrated by means of a realistic simulation example, which is also used to discuss future work.

Notation: For real vectors or matrices, ($'$) refers to their transpose. For symmetric matrices, ($\bullet$) denotes a symmetric block. The symbols $\mathbb{R}$, $\mathbb{R}_+$ and $\mathbb{N}$ denote the sets of real,

This research was supported by the "Coordenação de Aperfeiçoamento de Pessoal de Nível Superior (CAPES)", Finance Code 001, "National Council for Scientific and Technological Development (CNPq)", under grant numbers 303499/2018-4, and 303887/2014-1 and by São Paulo Research Foundation (FAPESP) under grant number 2017/20343-0.

Lucas N. Egidio, and Grace S. Deaecto ({egidio, grace}@fem.unicamp.br) are with School of Mechanical Engineering, UNICAMP, Brazil, João P. Hespanha (hespanha@ucsb.edu) is with Department of Electrical and Computer Engineering, University of California, Santa Barbara, USA, and José C. Geromel (geromel@dsce.fee.unicamp.br) is with School of Electrical and Computer Engineering, UNICAMP, Brazil.

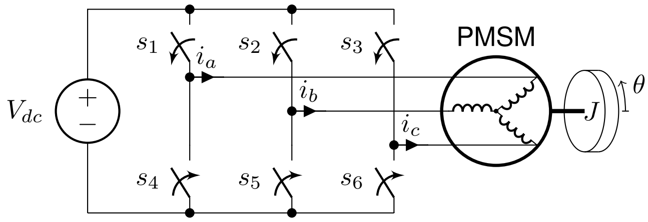

Fig. 1. PMSM and inverter schematic.

nonnegative real and natural numbers, respectively. The set $\mathbb{K} = \{1, \cdots, N\}$ is composed of the N first positive natural numbers. For real and symmetric matrix, $X > 0$ denotes a positive definite matrix. For a generic set $\mathbb{X}$ and a scalar $\alpha \in \mathbb{R}$, $\alpha\mathbb{X}$ denotes a set with all elements of $\mathbb{X}$ multiplied by $\alpha \in \mathbb{R}$. The convex combination of matrices with the same dimension is denoted as $X_\mu = \sum_{i\in\mathbb{K}} \mu_i X_i$ with $\mu \in \Lambda$ where $\Lambda \subset \mathbb{R}^N$ is the unit simplex.

II. PROBLEM FORMULATION

Consider a three-phase, two-poles PMSM fed by a three-phase voltage source inverter as depicted in Figure 1. This simplified schematics presents a DC link V_{dc}, six switches $\{s_1, \ldots, s_6\}$ and the PMSM. For the sake of simplicity, friction and external torques are neglected and the windings of all three phases are assumed to be identical. The coupled nonlinear differential equations governing the time evolution of the system are given by

$$L\frac{di_a}{dt} + Ri_a \;=\; v_a - \lambda_m \omega f_a(\theta) \tag{1}$$

$$L\frac{di_b}{dt} + Ri_b \;=\; v_b - \lambda_m \omega f_b(\theta) \tag{2}$$

$$L\frac{di_c}{dt} + Ri_c \;=\; v_c - \lambda_m \omega f_c(\theta) \tag{3}$$

together with

$$J\frac{d\omega}{dt} \;=\; \lambda_m i_a f_a(\theta) + \lambda_m i_b f_b(\theta) + \lambda_m i_c f_c(\theta) \tag{4}$$

$$\frac{d\theta}{dt} \;=\; \omega \tag{5}$$

where $i_a(t)$, $i_b(t)$ and $i_c(t)$ are phase currents, R and L stand, respectively, for each phase resistance and equivalent inductance, $v_a(t)$, $v_b(t)$ and $v_c(t)$ are the phase to neutral voltages, λ_m is the mutual flux linkage peak value, J is the rotor moment of inertia, $\theta(t)$ is the shaft angular displacement and $\omega(t)$ its angular velocity. The functions $f_a(\theta)$, $f_b(\theta)$ and $f_c(\theta)$ are related to the shape of the back electromotive force (back emf) along θ and are defined as

$$f_a(\theta) \;=\; \sin(\theta) \tag{6}$$

$$f_b(\theta) \;=\; \sin(\theta - 2\pi/3) \tag{7}$$

$$f_c(\theta) \;=\; \sin(\theta - 4\pi/3) \tag{8}$$

which we use to define the vector valued function $f(\theta) = [f_a(\theta)\ f_b(\theta)\ f_c(\theta)]' : \mathbb{R} \to \mathbb{R}^3$. We assume that each pair of adjacent switches is alternately commanded, for instance, when s_1 opens, s_4 closes and vice-versa. In view of this,

TABLE I

MODES σ, SWITCH STATES AND PHASE VOLTAGES, AS A FUNCTION OF THE STATES OF THE SWITCHES (s_i IS 1 WHEN THE SWITCH IS CLOSED AND 0 WHEN OPEN).

σ	s_1	s_2	s_3	v_a	v_b	v_c
1	0	0	1	-$V_{dc}/3$	-$V_{dc}/3$	2$V_{dc}/3$
2	0	1	0	-$V_{dc}/3$	2$V_{dc}/3$	-$V_{dc}/3$
3	0	1	1	-2$V_{dc}/3$	$V_{dc}/3$	$V_{dc}/3$
4	1	0	0	2$V_{dc}/3$	-$V_{dc}/3$	-$V_{dc}/3$
5	1	0	1	$V_{dc}/3$	-2$V_{dc}/3$	$V_{dc}/3$
6	1	1	0	$V_{dc}/3$	$V_{dc}/3$	-2$V_{dc}/3$
7	1 0	1 0	1 0	0	0	0

there exists a set of seven possible values for v_a, v_b and v_c, which are listed in Table I. This allows the definition of a switched nonlinear system with state space representation given by

$$\dot{x}(t) = A(\theta(t))x(t) + b_{\sigma(t)},\ x(0) = x_0 \tag{9}$$

where $x(t) = [i_a(t)\ i_b(t)\ i_c(t)\ \omega(t)]' : \mathbb{R}_+ \to \mathbb{R}^4$ is the state, and $\sigma(t) : \mathbb{R}_+ \to \mathbb{K} = \{1, \cdots, 7\}$ is the switching function to be designed, whose values correspond to the rows of Table I. The system matrices are defined as

$$A(\theta) = \begin{bmatrix} -(R/L)I_3 & -(\lambda_m/L)f(\theta) \\ (\lambda_m/J)f(\theta)' & 0 \end{bmatrix}, b_\sigma = \begin{bmatrix} (1/L)v_\sigma \\ 0 \end{bmatrix}$$

where $I_3 \in \mathbb{R}^{3\times3}$ denotes the identity matrix and the vector $v_{\sigma(t)} = [v_a(t)\ v_b(t)\ v_c(t)]' : \mathbb{R}_+ \to \mathbb{R}^3$ takes the values shown in Table I, for the different values of $\sigma(t)$. Notice that two configurations of switches produce mode $\sigma = 7$ with null phase voltages. We shall see that these null voltages could be ignored without loss of generality, since they can be determined by convex combinations of the other six operation modes.

The main goal of this paper is to design a state dependent function $u(x, \theta) : \mathbb{R}^4 \times \mathbb{R} \to \mathbb{K}$ such that the switching function $\sigma(t) = u(x(t), \theta(t))$ guarantees asymptotic convergence of the rotor velocity to a desired steady-state constant value ω^* and a guaranteed decay rate for the closed-loop system. Consider the bounded set

$$\Omega_\kappa = \{\omega \in \mathbb{R}\ :\ |\omega| \le \kappa\} \tag{10}$$

We assume that we have scalars $0 < \kappa^* \le \kappa$ to be determined in the sequel such that the steady-state velocity satisfies $\omega^* \in \Omega_{\kappa^*}$ and the velocity at each instant of time satisfies $\omega(t) \in \Omega_\kappa$ for all $t \in \mathbb{R}_+$.

A. Mathematical Properties of the Function $f(\theta)$

In view of (5), the shaft angle is given by

$$\theta(t) = \theta(0) + \int_0^t \omega(\tau)d\tau \tag{11}$$

which is fully defined by the forth state variable trajectory $\omega(t)$ and converges to the linear function $\theta^*(t) = cst + \omega^* t$ as t goes to infinity. Even though the trajectory of $\theta(t)$ is unbounded, the value of $f(\theta(t))$ is bounded for all $t \in$

$\mathbb{R}_+$. The vector valued function $f(\theta) : \mathbb{R} \to \mathbb{F} \subset \mathbb{R}^3$ has some particular properties that will be now discussed given their importance for our main results. First of all, notice that through trigonometric identities, it is possible to rewrite $f(\theta)$ as $f(\theta) = Gg(\theta)$ with

$$G = \begin{bmatrix} 1 & 0 \\ -1/2 & -\sqrt{3}/2 \\ -1/2 & \sqrt{3}/2 \end{bmatrix}, \quad g(\theta) = \begin{bmatrix} \sin(\theta) \\ \cos(\theta) \end{bmatrix} \tag{12}$$

where the matrix G represents the inverse Clarke transformation [9] and maps the phasor $g(\theta)$ from the $\alpha\beta$ reference frame to the abc frame. Two important characteristics of this matrix are that $G'G = (3/2)I_2$ and $e'G = 0$ where $e = [1\ 1\ 1]'$. Moreover, along trajectories $\theta(t)$, $\omega(t)$ of (5), we have that

$$g(\theta)'g(\theta) = 1, \quad \dot{g}(\theta)'g(\theta) = 0, \quad \dot{g}(\theta)'\dot{g}(\theta) = \omega^2 \tag{13}$$

Putting these properties together, it follows that

$$f(\theta)'f(\theta) = \frac{3}{2}, \quad \dot{f}(\theta)'f(\theta) = 0, \quad \dot{f}(\theta)'\dot{f}(\theta) = \frac{3}{2}\omega^2 \tag{14}$$

hold as well. Additionally, we have that $e'f(\theta) = 0,\ \forall\theta \in \mathbb{R}$. This means that the image of function $f(\theta)$ belongs to a plane orthogonal to the vector $e \in \mathbb{R}^3$, called the $\alpha\beta$ plane. In view of the fact that the Euclidean norm of $\|f(\theta)\| = \sqrt{3/2},\ \forall\theta \in \mathbb{R}$, we define the set where $f(\theta)$ is guaranteed to lie as

$$\mathbb{F} = \left\{ y \in \mathbb{R}^3 \ : \ e'y = 0,\ \|y\|^2 = 3/2 \right\} \tag{15}$$

which represents a circumference with radius $\sqrt{3/2}$ in the $\alpha\beta$ plane.

III. MAIN RESULTS

Within this section, we present the main results regarding the design of the switching function capable of assuring asymptotic stability of the switched nonlinear system (9) towards an equilibrium point $x_e = [0\ 0\ 0\ \omega^*]'$, with $\omega^* \in \Omega_{\kappa^*}$ given. First, we introduce the non-quadratic, radially unbounded, Lyapunov function candidate

$$\nu(x, \theta) = (x - x_e)'P(\theta)(x - x_e) \tag{16}$$

where the matrix valued function $P(\theta) : \mathbb{R} \to \mathbb{R}^{4\times4}$ is of the form

$$P(\theta) = \begin{bmatrix} pI_3 & \bullet \\ rf(\theta)' & q \end{bmatrix} \tag{17}$$

The real scalars (p, q, r) are design variables and their choice is linked to the switching function design. For an arbitrary trajectory $(x(t), \theta(t))$ of the system (1)-(5), one can show through straightforward but tedious algebraic manipulations that

$$\begin{aligned} \dot{\nu}(x, \theta) &= -(x - x_e)'Q(\theta, \omega)(x - x_e) + \\ &\quad +(c(\theta)(x - x_e))'(v_\sigma - \lambda_m f(\theta)\omega^*) \end{aligned} \tag{18}$$

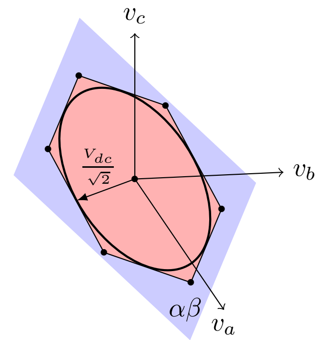

Fig. 2. Graphical representation of polytope $\mathbb{P}$ and inscribed circumference.

where the matrix valued functions $c(\theta) : \mathbb{R} \to \mathbb{R}^{3\times4}$ and $Q(\theta, \omega) : \mathbb{R} \times \mathbb{R} \to \mathbb{R}^{4\times4}$ are

$$\begin{aligned} Q(\theta, \omega) &= \begin{bmatrix} \frac{2R}{L}pI_3 - \frac{2\lambda_m}{J}rf(\theta)f(\theta)' & \bullet \\ \left(\frac{R}{L}r - \frac{\lambda_m}{J}q + \frac{\lambda_m}{L}p\right)f(\theta)' - r\dot{f}(\theta)' & \frac{3\lambda_m}{L}r \end{bmatrix} \\ c(\theta) &= \begin{bmatrix} \frac{2p}{L}I_3 & \frac{2r}{L}f(\theta) \end{bmatrix} \end{aligned}$$

The next theorem provides sufficient conditions for the existence of a switching rule that solves the previously stated problem.

Theorem 1: Let $\kappa^* \leq V_{dc}/(\sqrt{3}\lambda_m)$, $\omega^* \in \Omega_{\kappa^*}$ and $\kappa \geq \kappa^*$ be given. If there exist scalars (p, q, r) and $\eta > 0$ such that $Q(\theta(t), \omega(t)) > 2\eta P(\theta(t)) > 0$ for all $\theta(t) \in \mathbb{R}$ and $\omega(t) \in \Omega_\kappa$, then the switching function $\sigma(t) = u(x(t), \theta(t))$ with

$$u(x, \theta) = \arg\min_{i\in\mathbb{K}}(c(\theta)(x - x_e))'v_i \tag{19}$$

makes the equilibrium point x_e asymptotically stable and assures a decay rate of at least $\eta > 0$.

Proof: Recall that the function $f(\theta) : \mathbb{R} \to \mathbb{F}$ has an image given by a circumference in the $\alpha\beta$ plane. Since $e'v_i = 0$ for all $i \in \mathbb{K}$ then all vectors $v_i,\ i \in \mathbb{K}$, belong to the same plane in the $\mathbb{R}^3$. From this reasoning we are able to conclude that there exists a $\mu^* \in \Lambda$ satisfying $v_{\mu^*} = \lambda_m\omega^* f(\theta)$ for each $\theta \in \mathbb{R}$ if and only if

$$\lambda_m\omega^*\mathbb{F} \subseteq \mathbb{P} = \left\{ v \in \mathbb{R}^3 \ : \ v = \sum_{i\in\mathbb{K}} \mu_i v_i,\ \mu \in \Lambda \right\} \tag{20}$$

Considering that the greatest circle in the $\alpha\beta$ plane which is completely in the interior of the hexagonal polytope $\mathbb{P}$ has radius $V_{dc}/\sqrt{2}$ (see Figure 2), we obtain

$$v'_{\mu^*}v_{\mu^*} = (3/2)(\lambda_m\omega^*)^2 \leq V_{dc}^2/2 \tag{21}$$

which holds true because, by assumption, $\kappa^* \leq V_{dc}/(\sqrt{3}\lambda_m)$ and $\omega^* \in \Omega_{\kappa^*}$. Hence, taking into account the existence of $\mu^* \in \Lambda$, the equality (18) together with the switching rule (19) yield

$$\begin{aligned} \dot{\nu}(x, \theta) &= -(x - x_e)'Q(\theta, \omega)(x - x_e) + \\ &\quad +\min_{\mu\in\Lambda}(c(\theta)(x - x_e))'(v_\mu - \lambda_m f(\theta)\omega^*) \\ &< -2\eta(x - x_e)'P(\theta)(x - x_e) + \\ &\quad +(c(\theta)(x - x_e))'(v_{\mu^*} - \lambda_m f(\theta)\omega^*) \\ &= -2\eta\nu(x, \theta) \end{aligned} \tag{22}$$

for all (x,θ) such that $x \neq x_e$ and $\omega \in \Omega_\kappa$. The last equality holds from the fact that at each instant of time $t \in \mathbb{R}_+$ we are able to find a $\mu^* \in \Lambda$ such that $v_{\mu^*} = \lambda_m f(\theta)\omega^*$. The proof is concluded. ■

Through Theorem 1, asymptotic stability and a guaranteed decay rate can be imposed on the switching function design by choosing suitably the set of parameters (p,q,r) and $\eta > 0$. This is accomplished by guaranteeing that $P(\theta) > 0$ and $Q(\theta,\omega) > 2\eta P(\theta)$ for every $\theta \in \mathbb{R}$ and $\omega \in \Omega_\kappa$. A computationally intensive approach to this problem would exploit the periodicity of $f(\theta)$ by imposing these conditions on a sufficiently fine discrete grid of $\theta \in [0, 2\pi)$ and $\omega \in \Omega_\kappa$. However, a more sophisticated strategy can be adopted by using the result in the next lemma.

Lemma 1: Let the real parameters $(\alpha,\beta,\rho,\gamma,\psi)$ with $\beta \geq 0$ and $\kappa > 0$ be given. The matrix valued function $S(\theta,\omega) : \mathbb{R} \times \mathbb{R} \to \mathbb{R}^{4\times 4}$ defined by

$$S(\theta,\omega) = \begin{bmatrix} \alpha I_3 - \beta f(\theta) f(\theta)' & \bullet \\ \rho f(\theta)' - \gamma \dot{f}(\theta)' & \psi \end{bmatrix} \tag{23}$$

is positive definite for all $\theta(t) \in \mathbb{R}$ such that $\omega(t) \in \Omega_\kappa$ if and only if the following conditions

$$2\alpha/3 > \beta, \;\; 2\psi/3 > \left(\frac{\gamma^2}{\alpha}\right)\kappa^2 + \left(\frac{\rho^2}{\alpha - 3\beta/2}\right) \tag{24}$$

hold simultaneously.

Proof: Since by assumption $\beta \geq 0$ then the first diagonal matrix block of $S(\theta,\omega)$ is positive definite if and only if

$$\begin{bmatrix} \alpha I_3 & \bullet \\ \sqrt{\beta} f(\theta)' & 1 \end{bmatrix} > 0 \tag{25}$$

and the Schur Complement with respect to the first diagonal element indicates that this holds if and only if $\alpha > 0$ and $1 > (\beta/\alpha) f(\theta)' f(\theta) = 3\beta/(2\alpha)$ which is exactly the first condition in (24). Using this fact, the Schur Complement of (23) with respect to the first diagonal element indicates that $S(\theta,\omega)$ is positive definite if and only if

$$\psi > (\rho f(\theta) - \gamma \dot{f}(\theta))' (\alpha I_3 - \beta f(\theta) f(\theta)')^{-1} (\rho f(\theta) - \gamma \dot{f}(\theta)) \tag{26}$$

Using the Matrix Inversion Lemma, see [13], it follows that

$$(\alpha I_3 - \beta f(\theta) f(\theta)')^{-1} = \frac{1}{\alpha} I_3 + \frac{\beta}{\alpha} \left(\frac{f(\theta) f(\theta)'}{\alpha - 3\beta/2} \right) \tag{27}$$

which can be used in (26) together with (14) to obtain

$$\begin{aligned} \psi &> 3\rho^2/(2\alpha) + 3\gamma^2\omega^2/(2\alpha) + (\beta/\alpha)\left(\frac{(3/2)^2 \rho^2}{\alpha - 3\beta/2}\right) \\ &= 3\gamma^2\omega^2/(2\alpha) + \left(\frac{(3/2)\rho^2}{\alpha - 3\beta/2}\right) \end{aligned} \tag{28}$$

which is verified for all $\omega \in \Omega_\kappa$ if and only if the second inequality in (24) holds, thus concluding the proof. ■

This result enable us to establish conditions under which the inequalities $Q(\theta,\omega) > 2\eta P(\theta) > 0$ hold for all $\theta \in \mathbb{R}$ and $\omega \in \Omega_\kappa$.

Corollary 1: Let $\kappa > 0$ be given. The parameters (p,q,r) and $\eta > 0$ solution of the optimization problem

$$\max_{\eta > 0} \{\eta : Q(\theta,\omega) > 2\eta P(\theta) > 0, \; \forall \theta \in \mathbb{R}, \forall \omega \in \Omega_\kappa\} \tag{29}$$

are equivalently determined by the following generalized eigenvalue problem

$$\max_{p,q,r,\eta>0} \quad \eta \tag{30}$$

subject to

$$\mathcal{P} = \begin{bmatrix} 2q/3 & \bullet & \bullet \\ 0 & p & \bullet \\ r & 0 & p \end{bmatrix} > 0 \tag{31}$$

$$\begin{bmatrix} 2\frac{\lambda_m}{L} r & \bullet & \bullet \\ \kappa r & 2\frac{R}{L} p & \bullet \\ \frac{R}{L} r - \frac{\lambda_m}{J} q + \frac{\lambda_m}{L} p & 0 & 2\frac{R}{L} p - 3\frac{\lambda_m}{J} r \end{bmatrix} > 2\eta \mathcal{P} \tag{32}$$

Proof: First, notice that the conditions (24) can be expressed in terms of a linear matrix inequality of the form

$$\begin{bmatrix} 2\psi/3 & \bullet & \bullet \\ \kappa\gamma & \alpha & \bullet \\ \rho & 0 & \alpha - 3\beta/2 \end{bmatrix} > 0 \tag{33}$$

Now, making $S(\theta,\omega) = P(\theta)$, Lemma 1 assures that inequality (31) is equivalent to $P(\theta) > 0$ for all $\theta \in \mathbb{R}$. In the same manner, writing $S(\theta,\omega) = Q(\theta,\omega) - 2\eta P(\theta)$, Lemma 1 assures that inequality (32) is equivalent to $Q(\theta,\omega) > 2\eta P(\theta)$ for all $\theta \in \mathbb{R}$ and $\omega \in \Omega_\kappa$. ■

Notice that the generalized eigenvalue problem stated in this corollary has global optimal solution efficiently provided by off-the-shelf tools, see [2]. For this specific problem the designer can, without any loss of generality, fix one of the parameters of $P(\theta)$, for instance $q = 1$, normalizing the constraints and reducing the problem order. Moreover, problem (30) always accepts a feasible solution since $p = (L/J)q > 0$ and small enough parameters $r > 0$ and $\eta > 0$ verify both linear inequalities (31)-(32).

Finally, it is important to mention that from Theorem 1, the decay rate $\eta > 0$ allows to conclude that $\omega(t) \in \Omega_\kappa, \forall t \in \mathbb{R}_+$, is always satisfied provided that $\kappa \geq \kappa^*$ is chosen large enough and $\omega(0)$ belongs to a pre-specified subset of Ω_κ. However, since in general the optimal objective function (30) decreases as κ increases, this design parameter must be determined with particular attention. This aspect is illustrated in the next section.

IV. SIMULATION RESULTS

This section is devoted to present a practical example whose switching function is designed through the previous results in order to control the rotational velocity of a PMSM. The considered parameters were borrowed from [14] and are given by: $R = 0.665$ ohm, $L = 1.113$ mH, $\lambda_m = 0.0167$ V·s/rad, $J = 2$ mg·m^2 and $V_{dc} = 24$ V. Since $\kappa^* \leq V_{dc}/(\sqrt{3}\lambda_m) = 829.7249$ rad/s we have adopted $\kappa^* = 418.879$ rad/s (or 4000 rpm). To investigate the effect of the stability domain definition on the maximum guaranteed decay rate, the optimization problem (30) was

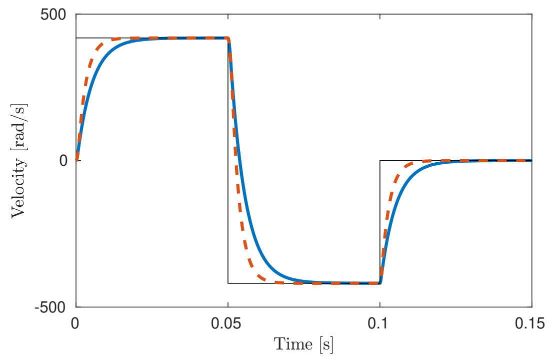

Fig. 3. Velocity ω and reference ω^* (black) for $\mathcal{S}_1$ (solid) and $\mathcal{S}_2$ (dashed).

solved for several values of $\kappa \geq 0$ and, as expected, it has been verified that η is a decreasing function of κ, i.e., the decay rate increases when the stability domain decreases leading, in general, to faster settling times.

Solving the problem (30) for $\kappa = 829.7249$ rad/s, we have found the solution set $\mathcal{S}_1$, composed of $p_1 = 504.4854$, $r_1 = 8.0283$ and $q_1 = 1$, together with the decay rate $\eta_1 = 99.8552$ Hz. A second solution set for (30) which considers $\kappa = \kappa^*$, is defined as $\mathcal{S}_2$ with $p_2 = 424.9550$, $r_2 = 12.7189$, $q_2 = 1$ and the decay rate $\eta_2 = 219.3554$ Hz.

For both solution sets, a numerical simulation starting from null initial conditions was conducted considering $\omega^* = 418.879$ rad/s when $t \in [0, 0.05)$, $\omega^* = -418.879$ rad/s when $t \in [0.05, 0.10)$ and $\omega^* = 0$ rad/s when $t \in [0.10, 0.15)$. Figure 3 depicts the rotational velocity trajectories where it is noticed that $\omega(t) \in \Omega_\kappa$ for all $t \in [0, 0.15]$ as required. Furthermore, it is seen that $\omega(t) \in \Omega_{\kappa^*} \subset \Omega_\kappa$ in the same time interval. Figure 4 shows the correspondent phase currents over time. The switching signals generated by the switching function (19) are shown in Fig. 5. These simulations allow us to conclude that adopting the solution set $\mathcal{S}_1$, the angular velocity attains 98% of the desired reference value in ≈ 20 ms while the one associated with $\mathcal{S}_2$ attains it in ≈ 11 ms, confirming the previous discussions.

A. Application to a Brushless DC Motor

Brushless DC machines (BLDCM) differs from PMSM mainly by the shape of the back emf where, instead of a sinusoidal pattern, they present a trapezoidal one [15]. However, we will now extrapolate the design conditions presented here to deal with BLDCM using the fact that a sinusoidal function is a fair approximation to a trapezoidal one and can be obtained from the first term of the Fourier series. Figure 6 presents the considered normalized trapezoidal back emf $f_t(\theta)$ along with its fundamental approximation $\tilde{f}_t(\theta) = 1.2159 \sin(\theta)$.

Replacing the vector function $f(\theta)$ in (9) by $[f_t(\theta)\ f_t(\theta - 2\pi/3)\ f_t(\theta - 4\pi/3)]'/1.2159$ and running again the previous simulation for the same switching function, almost identical trajectories were obtained, letting us conclude that the technique is robust with respect to the back emf shape. The figures were omitted due to limited space.

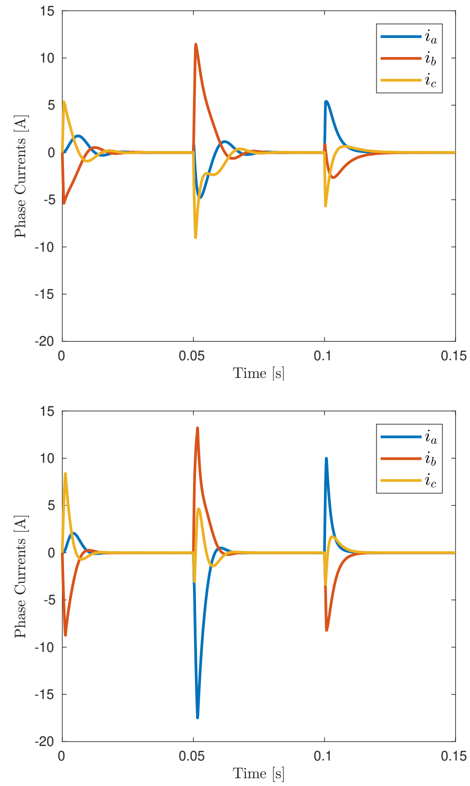

Fig. 4. Phase currents for $\mathcal{S}_1$ (top) and $\mathcal{S}_2$ (bottom).

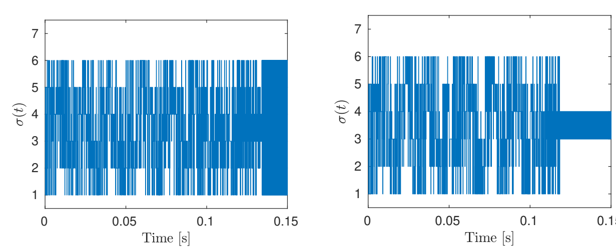

Fig. 5. Switching signal $\sigma(t)$ for $\mathcal{S}_1$ (left) and $\mathcal{S}_2$ (right).

B. Dwell-time and friction effects

We now explore the effects of the presence of dwell-time and viscous friction by means of numerical simulations. Taking into account the switching function associated with the solution set $\mathcal{S}_2$, we carried out simulations, first considering a viscous friction on the rotor shaft of intensity $c \geq 0$ replacing (4) by

$$J\frac{d\omega}{dt} + c\omega = \lambda_m i_a f_a(\theta) + \lambda_m i_b f_b(\theta) + \lambda_m i_c f_c(\theta)$$

and latter a dwell-time T, representing the amount of time that the controller output must remain constant between two consecutive switching instants. The rotor velocity $\omega(t)$ is plotted in Figure 7 for different values of c and T.

These data corroborate the need for more investigation regarding the presented approach as it is clear that these ignored phenomena can drastically affect the performance of the system as their intensities increase.

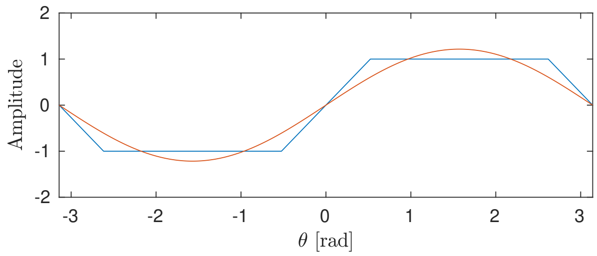

Fig. 6. Trapezoidal back emf $f_t(\theta)$ (blue) and approximation $\tilde{f}_t(\theta)$ (red).

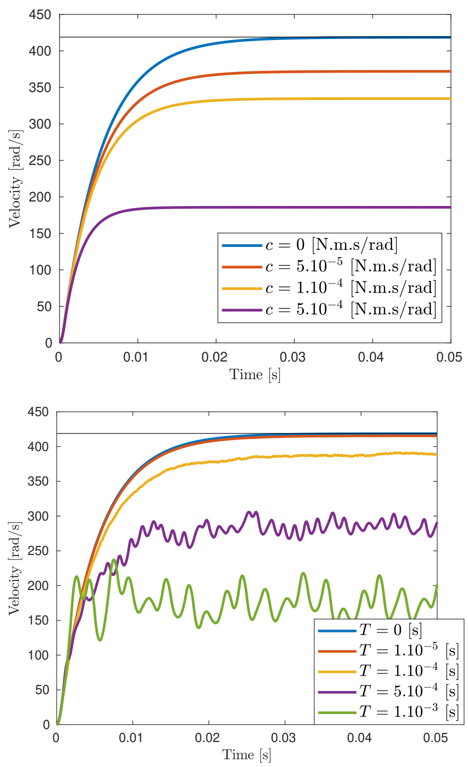

Fig. 7. Effect of different levels of viscous friction and dwell-time values.

V. CONCLUSIONS AND FUTURE WORKS

A new approach, based on the design of a switching function to asymptotically control the rotational velocity of a PMSM fed by a three-phase inverter was presented. This methodology, to the best of the authors knowledge, is the first one allowing for the switched systems framework without considering any reference transformation and using a single control loop. The switching function is simple to be implemented requiring a look-up table for evaluating the sinusoidal vector function $f(\theta)$ and some basic addition and multiplication operations. Despite the nonlinear nature of the system, the design conditions are given in terms of a generalized eigenvalue problem that can be easily solved in polynomial time by means of available optimization solvers. Moreover, these conditions assure an optimized decay rate inside a predefined stability domain. A simulation was presented to verify that the proposed technique is indeed valid and efficient to control the rotor velocity to a desired steady-state value, even when a trapezoidal back emf, as the one in BLDCM, was considered.

Taking into account the external torque and various kinds of friction are practical issues to be studied in future work. Also, the consideration of dwell-time must be investigated as it is well known that high frequency switching is a source of losses in power devices. Studies about the passivity and the generic behavior of these machines, working as motors or generators, are also of interest together with extensions to different electric drives such as induction and synchronous AC machines. The optimization of performance measures such as the L_2 norm is also to be addressed. Additionally, switching algorithms based on an output feedback rather than state feedback would simplify and reduce costs in practical implementations, where the use of sensors is usually undesirable.

REFERENCES

[1] P. Bolzern and W. Spinelli. Quadratic stabilization of a switched affine system about a nonequilibrium point. In *IEEE American Control Conference, 2004*, volume 5, pages 3890–3895, 2004.

[2] S. Boyd, L. El Ghaoui, E. Feron, and V. Balakrishnan. *Linear Matrix Inequalities In System and Control Theory*, volume 15. SIAM, 1994.

[3] D. Casadei, F. Profumo, G. Serra, and A. Tani. FOC and DTC: two viable schemes for induction motors torque control. *IEEE Transactions on Power Electronics*, 17(5):779–787, 2002.

[4] D. Corona, J. Buisson, B. De Schutter, and A. Giua. Stabilization of switched affine systems: An application to the buck-boost converter. In *IEEE American Control Conference, 2007.*, pages 6037–6042, 2007.

[5] G. S. Deaecto. Dynamic output feedback $\mathcal{H}_\infty$ control of continuous-time switched affine systems. *Automatica*, 71:44–49, 2016.

[6] G. S. Deaecto and J. C. Geromel. Stability analysis and control design of discrete-time switched affine systems. *IEEE Transactions on Automatic Control*, 62(8):4058–4065, 2017.

[7] G. S. Deaecto, J. C. Geromel, F. Garcia, and J. Pomilio. Switched affine systems control design with application to dc–dc converters. *IET Control Theory & Applications*, 4(7):1201–1210, 2010.

[8] R. A. DeCarlo, M. S. Branicky, S. Pettersson, and B. Lennartson. Perspectives and results on the stability and stabilizability of hybrid systems. *Proceedings of the IEEE*, 88(7):1069–1082, 2000.

[9] W. C. Duesterhoeft, M. W. Schulz, and E. Clarke. Determination of instantaneous currents and voltages by means of alpha, beta, and zero components. *Transactions of the American Institute of Electrical Engineers*, 70(2):1248–1255, 1951.

[10] L. N. Egidio, H. R. Daiha, G. S. Deaecto, and J. C. Geromel. Dc motor speed control via buck-boost converter through a state dependent limited frequency switching rule. In *IEEE 56th Annual Conference on Decision and Control (CDC), 2017*, pages 2072–2077, 2017.

[11] L. N. Egidio and G. S. Deaecto. Novel practical stability conditions for discrete-time switched affine systems. *IEEE Transactions on Automatic Control*, to appear, 2019.

[12] J. C. Geromel and P. Colaneri. Stability and stabilization of continuous-time switched linear systems. *SIAM Journal on Control and Optimization*, 45(5):1915–1930, 2006.

[13] R. A. Horn and C. R. Johnson. *Matrix Analysis*. Cambridge university press, 1990.

[14] K. Jezernik, J. Korelič, and R. Horvat. PMSM sliding mode FPGA-based control for torque ripple reduction. *IEEE Transactions on Power Electronics*, 28(7):3549–3556, 2013.

[15] R. Krishnan. *Permanent Magnet Synchronous and Brushless DC Motor Drives*. CRC press, 2009.

[16] D. Liberzon. *Switching in Systems and Control*. Birkhauser, 2003.

[17] Z. Sun and S. S. Ge. *Stability theory of switched dynamical systems*. Springer Science & Business Media, 2011.

[18] A. Trofino, D. Assmann, C. C. Scharlau, and D. F. Coutinho. Switching rule design for switched dynamic systems with affine vector fields. *IEEE Transactions on Automatic Control*, 54(9):2215–2222, 2009.

[19] L. Zhong, M. F. Rahman, W. Y. Hu, and K. Lim. Analysis of direct torque control in permanent magnet synchronous motor drives. *IEEE Transactions on Power Electronics*, 12(3):528–536, 1997.